academicJournals

Vol. 12(41), pp. 6032-6041, 9 October, 2013
DOI: 10.5897/AJB2012.12.3024
ISSN 1684-5315 ©2013 Academic Journals
http://www.academicjournals.org/AJB

African Journal of Biotechnology

Full Length Research Paper

Morphology and anatomical structure of the larval salt gland of *Artemia tunisiana* under different salinities

Magdy E. Mahfouz[1], Mona M. El-Gamal[2*] and Suzan M. Shraby[1]

[1]Department of Zoology, Faculty of Science, Kafrelsheikh University, Egypt.
[2]Department of Zoology, Faculty of Science, Tanta University, Egypt.

Accepted 16 September, 2013

Brine shrimps of the genus *Artemia* is characterized by its high adaptability to adverse environmental conditions. To elucidate the effect of salinity on the neck organ (salt gland) of *Artemia tunisiana* nauplii, the morphology and fine structure of the ion transporting epithelium were examined following culturing under different salinities (25, 40, 70, 140 and 180 g/L). The expression of APH-1 mRNA, using semi-quantitative reverse transcription-polymerase chain reaction (RT-PCR), was also determined. The morphology and anatomical structure of the salt gland varied according to the salinity degree. At low salinities, salt gland was small, thin and flat having many shallow canals, while at high salinities, it was more elongated with deeper canals and grooves. Ultrastructure examination showed low amplification of the plasma membrane at 25 g/L with no tubular tufts, while at 40 and 70 g/L salinities, the apical and central zones showed a large amplification of the surface area of the plasma membrane. At 140 g/L salinity, the epithelial cells were more elongated and the cuticle appeared to be composed of many layers. The general structure of the salt gland of nauplii cultured at 180 g/L disappeared. Semi-quantitative APH-1 mRNA analysis indicated that the gene was expressed in all tested salinities. The expression did not change remarkably between 25 and 40 g/L salinities. As salinity increased, the gene was up regulated at 70 g/L and reached the highest level at 140 g/L, while the expression level reduced significantly at 180 g/L. This coincides with the histological results and highlights the possible role of APH-1 in salinity protection in *Artemia.*

Key words: *Artemia*, nauplii, salt gland, salinity, APH-1 gene expression

INTRODUCTION

Salinity is one of the most important physical parameters affecting the life history of hypersaline organisms like *Artemia*. Genus *Artemia*, subdivided into six generally recognized bisexual species and a large number of parthenogenetic populations, is characterized by its adaptability to a wide range of salinity; 4 to 250 g/L (Varo et al., 2002). The ability of brine shrimp *Artemia* to exist in a broad salinity range results from an active excretion of sodium ions from the body into the external environment (Conte et al., 1972). The extent to which *Artemia* can tolerate extremes of salinity is evident in Wadi El-Natrun and Borg El-Arab, where both larvae and adults may be observed swimming amongst crystals of NaCl in saturated brine. Two structures seem to be actively involved in the osmoregulatory abilities of the adults, the epithelium of the gut (Croghan, 1958) and the metepipodite segments of the branchiae (Copeland, 1966). In *Artemia* nauplii, there is a lack of gut and metepipodites because at this stage of embryonic development, the analog of the legs segments have not formed their definitive structures. Nevertheless, nauplii possess a unique structure for coping with salinity differences via a larval salt gland or neck organ. This gland has been most thoroughly described for larval anostracans, because it is

*Corresponding author. E-mail: Drmona2005@hotmail.com.

primarily a larval organ and because of the amount of attention lavished on the developmental biology of the genus *Artemia* (Criel, 1991). The salt gland in anostracans has been known since 1851 when Leydig described it in *Artemia salina*. Afterward, researchers described this structure in adults and in larvae (Sars, 1896 and Schrehardt, 1986), while others restricted the presence of salt gland in larvae of anostracans and its disappearance by the adult stage (Schrehardt, 1987). This structure is also known from notostracans, conchostracans and many species of cladocerans (Fryer, 1987; Martin and Laverack, 1992). The morphology and ontogeny of the gland were reviewed by Criel (1991); his description is based on the earlier work by Conte et al. (1972), Ewing et al. (1974) and Hootman and Conte (1975). Beside its role in ionic and osmotic regulation, other functions have been suggested for the salt gland including: (1) Adherence to external objects (Zenker, 1851), (2) respiration (Dejdar, 1930) and (3) support for the antennal and mandibular muscles (Weisz, 1947). Conte et al. (1972) found that larval brine shrimp like their adult counterparts are capable of living in saturated brines because they possessed this special organ that is capable of providing osmotic and ionic regulation (Hootman et al. 1972; Criel, 1991). Abel and Ellis (1966) investigated the need for such an organ. This function was supported by micropuncture studies (Russler and Mangos, 1978) and by the finding of Na^- K^- activated ATPase in the organ (Conte et al., 1977). All of them concluded that, brine shrimp use salt gland pump to maintain a relatively stable salt concentration within their bodies.

Artemia posses a drifter gene, designated *APH*-1 for *Artemia* POU-Homeoprotein, which is proved to be expressed in the salt gland (Chavez et al., 1999). This gene encodes a POU-III subclass homeobox-containing transcription factor highly related to the Drosophila drifter (Dfr) protein (Anderson et al., 1996). One prominent role of such gene is controlling tracheal development and transcription factor (Zelzer and Schilo, 2000) in addition to its possible role in salt regulation (Wang et al., 2012). Despite its early recognition, little definitive data concerning the morphology of the salt gland in *Artemia tunisiana* as well as the changes in gene expression due to culturing under different salinities. The herein work represents the results of light and electron microscopic study of the morphology and anatomy of the salt gland epithelium beside molecular expression of APH-1 in *Artemia* cultured under different salinities to understand the impact of this environmental stressor on the structure and function of *Artemia* salt gland.

MATERIALS AND METHODS

Collection of cysts

Local *Artemia* cysts were collected from inland saline lake Wadi El-Natrun situated in northern Egypt (30° 10′ N, 30° 27′ E). Cysts were stored and transported to the laboratory in plastic bags, then cleaned and dried using the bi-flotation technique described by Sorgeloos (1978). The dried cysts were stored at -20°C.

Culture techniques

The dried cysts were hydrated in a solution of instant Ocean Sea salt (40 g/L) at 28°C with continuous aeration. Approximately 20 to 24 h were needed for hatching at this temperature. Newly hatched nauplii (2000 to 2500 individuals) were transferred to 2 L culture flasks containing the different salinity experimental media (25, 40, 70, 140 and 180 g/L) made up with Ocean Sea salt and autoclaved deionized water. All cultures were kept at 28°C with continuous illumination and aeration. *Artemia* in each culture was fed with yeast and the culture medium was replaced every four days. When *Artemia* specimens reached the pre-adult stage (≈3 mm in length) their concentration was adapted to 100 individuals/flask, till reproductive time (when males are clasping females) as the number was adjusted to 10 couples/ flask. The first generation from the above cultures was collected. In the cases of 25, 40 and 70 g/L salinities, nauplii were immersed directly in the cultures, while at 140 and 180 g/L salinities, cysts were collected, dried and then hatched in the salinity experimental media as their parents. This gradual accommodation gives a depiction about what really happens in nature.

According to Weisz (1947) scheme, in which developmental stage is quantitatively assessed by the number of body segments present, stages 3-5 were used in this study (48 h post hydration). *Artemia* samples were either; collected and frozen (-80°C) in view of extracting RNA or processed for microscopy preparation.

Light and electron microscopy preparations

Nauplii were removed with disposable pipettes and placed on a rubber stopper under a dissecting microscope. The abdomen of each nauplius just posterior to the margin of the thoracic segments was removed using a fine metal needle to facilitate rapid fixation. The nauplii were transferred to a fixative solution [6% glutaraldehyde in 0.2M, S-collidine (pH 7.5) with 8.6% sucrose and a trace (0.002%) of $CaCl_2$] at 4°C as suggested by Bell et al. (1969). After 24 h, postfixation was carried out in 1% solution of OsO_4 in 0.2 M sodium phosphate (pH 7.4) with 20% sucrose at room temperature (26°C). The specimens were dehydrated through a graded series of ethanol (30-100%), transferred through propylene oxide and gradually embedded in Epon/Araldite resin mixture. Ultra-thin sections (0.5 µm) were cut on ultramicrotome and mounted. Some sections were mounted on glass slides and stained with methylene blue-azure II for light microscopic examination. The rest of sections were mounted on copper grids and stained with aqueous uranyl acetate for 30 min and lead citrate for 5 min. These sections were examined and photographed at a JEOL 100 Transmission Electron Microscope.

RNA extraction and reverse transcription-polymerase chain reaction (RT-PCR)

Total RNA was isolated from three *Artemia* nauplii from each of the examined salinities using Trizol reagent (Invitrogen). All dissecting equipment and homogenizers were cleaned with RNAse-Zap (Ambion, Austin, TX, USA) and rinsed in RNAse-free water in order to work under RNAse-free conditions. Total RNA concentration, as well as the integrity and purity of each sample were determined to ensure the lack of genomic DNA contamination.

Of each sample, 1.5 µg RNA was reverse transcribed into complementary DNA (cDNA) in a volume of 25 µl of reaction mixture

containing random hexanucleotides primer (0.2 µg/reaction), deoxyribonucleotide triphosphate (dNTP-0.5 mM of each), avian myeloblastosis virus reverse transcriptase (RT, AMV) (20 units/reaction), RNasin (20 units/reaction) and 2.5 µl of 10x PCR buffer. After an initial 5 min at 70°C in order to dissociate secondary RNA structures, samples were incubated at 42°C for 60 min. Reactions were terminated after 5 min at 95°C.

PCR was performed initially using primers for *Artemia* mitochondrial 16S rRNA (Palmero et al., 1988) (sense, 5′-AACAGACGCCTCTCTAGGCT-3′; antisense, 5′-CTTAAATGTACTTGGAGGGCG-3′), which served as a positive control for RT-PCR due to its constitutive expression. Products obtained using 20 cycles of amplification were within the linear range of signal amplification and allowed titration of the amount of template to be subsequently used in order to obtain consistent amounts of product between samples. The adjusted cDNA volumes were then used in the succeeding PCR reactions employing gene-specific primers for APH-1 (sense, 5′-AGTGCAGTCAGTTCTGAACCG-3′; antisense, 5′-GGGTACCATTCAAGGAGTCTC-3′) (Chavez et al., 1999). All specific primers were synthesized by Sigma-Aldrich (USA). Negative control reactions were performed either without cDNA template in order to ensure that no products arose due to contamination or primer-dimer effects, or with adults *Artemia* that are expected to lack the APH-1 transcription at this stage (Chavez et al., 1999).

The PCR reaction mixture was set up in a total volume of 50 µl, containing 2 µl of reverse transcriptase product, 5 µl of a 10x PCR standard buffer, 1.5 µl 50 mM MgCl2, 1 µl 10 mM dNTP mix, 1.5 units Taq DNA polymerase (Promega) and the selected primer pair (20 pmol/primer/reaction). For both APH-1 mRNA and mt 16S rRNA, amplifications were performed using 35 cycles of denaturation (1 min at 95°C), annealing (1 min at 58°C), and extension (2 min at 72°C) followed by a final extension at 72°C for 10 min. Denaturation for 5 min at 95°C preceded cycling.

Semi-quantitative analysis of gene expression

Following PCR, a 10-µL aliquot of each PCR product was analyzed by electrophoresis on 1.5% agarose gel containing ethidium bromide and the bands were visualized in a UV- transilluminator for the presence of amplified DNA. Semi-quantitative assessments of mRNA levels were determined by quantifying the intensity of each band of PCR product through using Gel Analyzing Imager (Sharp-100). This relies on the quantification of the investigated genes expression on the basis of optical density of detected bands. The relative intensity of APH-1 to that of 16S rRNA was then determined. Corrected values were obtained by dividing the measured value for APH-1 by that of 16S rRNA. Mean values of three measurements of APH-1 expression relative to the corresponding 16S rRNA expression are presented.

RESULTS

General salt gland morphology

The salt gland of *Artemia* cultured at any investigated salinity was distinguished in early developmental stages; it was located on the mid line of the anterior head region, often just posterior to the eyes. The organ usually demarcated from the surrounding cuticle by thin cuticular festoon border and slightly elevated with respect to the surrounding cuticle. Irregular grooves extended throughout the gland surface and distinguished this area from the rest of the surface of the nauplius (Figure 1). With increasing salinity, the salt gland became enlarged and acquired different shape with several kinds of surface irregularities

At 25 g/L salinity

The salt gland was thin flat cap like structure; its diameter ranged from 117-160 µm and had many superficial canals (Figure 1A).

At 40 g/L salinity

The salt gland measured between 138-180 µm across the diameter of the circular base. The epithelium changed from a flat cap like structure into a hemispherical dome having more channels through the epithelium (Figure 1B).

At 70, 140 and 180 g/L salinities

At these high salinities, there were more development and growth of the gland (Figure 1C-F). The canals and grooves were deeper with the salinity increment. Also these grooves distinguished salt gland from the rest of the surface of the nauplius and transformed the gland from a smooth overlay into a covering that was mottled in appearance. The removal of the cuticular layer from the gland showed the secretory epithelium to have a striking surface pattern as illustrated in Figures 1E and F in nauplii cultured at 140 and 180 g/L salinities.

Histological and ultrastructure investigations

Histological investigation

Semi-thin sections of salt glands in nauplii cultured under different salinities showed a single layer of cuboidal-columnar epithelial cells. At 25 g/L salinity as illustrated in Figure 2A, the epithelial cells ranged from 23 to 45 cells with a diameter ranged from 20-28 µm from the apical (cuticular) to the basal surface (haemocoelic). The number of epithelial cells in those cultured at 40 and 70 g/L increased to become 35 to 52 cells with a diameter ranged from 26 to 32 µm (Figure 2B). With the elevation of salinity (140 and 180 g/L), the number of epithelial cells decreased (28 to 42 cells). The central portion of the salt gland was occupied with few scattered cells, characterized by many vacuoles especially in nauplii cultured at 180 g/L salinity (Figure 2C). In all cases, no boundaries between cells were distinct.

Ultrastructure investigations

Salt gland in nauplii cultured at 25, 40, 70, 140 g/L Salinity evidenced three zones; apical, central and basal

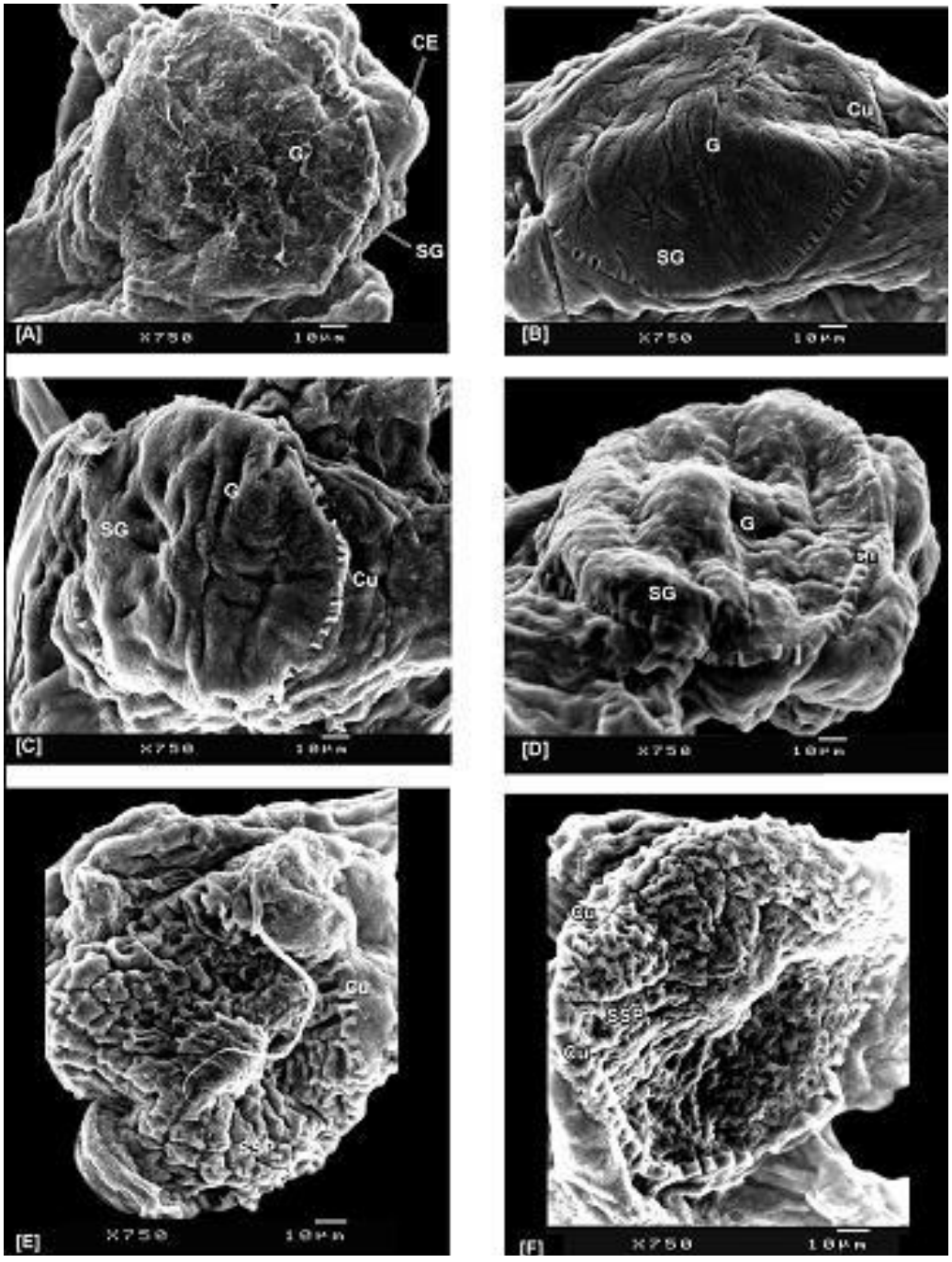

Figure 1. SEM photographs of salt gland of *Artemia tunisiana* (A-E stage 3 and F stage 5) at (A) 25 g/L, (B 40 g/L), (C) 70 g/L (D and E) 140 g/L and (F) at 180 g/L salinity, (E and F), the culticular layer has been removed during preparation. CE, compound eye; Cu, cutucus; G, groove; SG, salt striking surface pattern.

zone, while those cultured at salinity 180 g/L missed the previous zones pattern in both thickness and structure.

At 25 g/L salinity: Under the mentioned salinity the apical and central zones showed low amplification of the surface area of the plasma membrane (Figure 3A). The first pattern evolved from the plasma membrane was located at the apical surface and did not form tubular tufts beneath the cuticular surface as the other salinities. The second pattern formed smooth endoplasmic reticulum (labyrinth) which filled the central cytoplasmic zone. This

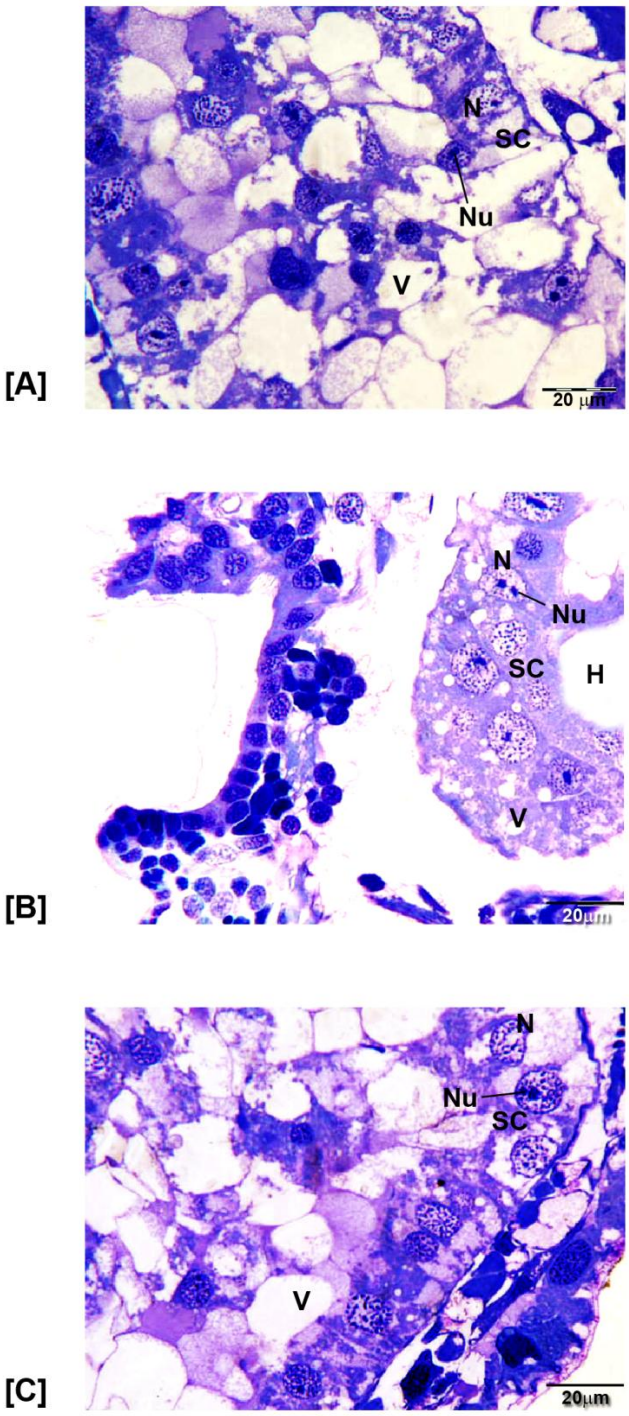

Figure 2. Light micrographs of semi-thin sections of salt gland epithelia (stage 3) cultured at A, 25 g/L; B, 40 g/L; C, 180 g/L sality. H, Haemocoeil; N, nucleus; Nu, nucleolus; SC, scattered cells; V, vacuoles.

network appeared to be composed of tubules of undetermined length and extended to the basal cell surfaces. Labyrinthine channels occupy the spaces between adjacent nuclei and form sinusoids open directly into the haemocoel. The central zone was characterized by an abundance of oval or round mitochondria. The basal zone contained most of the nuclei along with yolk platelets that vary greatly in size (2-6 µm in diameter) and other storage products. Nuclei were large, roughly oval, and contain intensely staining nucleoli and chromatin. The number of nucleoli visible may range from one to three. The entire epithelial complex of the gland did not rest upon a basal lamina. Other organelles as Golgi apparatus and membrane-bound vesicles were present.

At 40 g/L salinity: The apical and central zones showed a large amplification of the surface area of the plasma membrane. Two patterns have evolved from the surface boundary of the plasma membrane; the first (tubular tufts) located at the apical surface extended into large numbers of irregular shaped projection forming tubular tufts that lie beneath the cuticular surface. The second was the ramified network of smooth endoplasmic reticulum (labyrinth) which filled the central cytoplasmic zone. This network appeared to be composed of tubules of undetermined length and extended to the basal cell surfaces. Labyrinthine channels also occupied the spaces between adjacent nuclei and formed sinusoids that open directly into the haemocoel (Figure 3B). The tubular tufts did not associate with the mitochondria. The central zone was characterized by an abundance of mitochondria, while the basal zone contained most of the nuclei along with yolk platelets. Nuclei were large, roughly oval, and contain intensely staining nucleoli and chromatin.

At 70 g/L salinity: The salt glands structure of nauplii cultured under 70 g/L salinity resembled those cultured at 40 g/L salinity with more amplification of the apical and central zones (Figure 3C). Mitochondria were the most abundant organelles, they were oval or round and distributed throughout the cells, but were numerous in the labyrinth. Mitochondria (single or aggregated) were found to be closely associated with the tubules of the labyrinth. Single mitochondrion appeared to be enclosed in capsule-like extensions of cytoplasm, while aggregated ones were separated from each other by a narrow canaliculus (Figure 3D). Cristae were numerous and iregular. Other organelles as Golgi apparatus and membrane-bound vesicles were present.

At 140 g/L salinity: The epithelial cells were more elongated (Figure 4A) than those cultured under lower salinities. The cuticle appeared to be composed of many layers and not two as in the case of salt glands cultured under other investigated salinities (25, 40 and 70 g/L). The thickness of the cuticle layer increased to 30-42 nm. The apical plasmalemma showed minor infolding and some areas exhibited blocks of tubules (Figure 4B). Nuclei were elongated and contained intensely staining hetero-chromatin. The central zone was characterized by

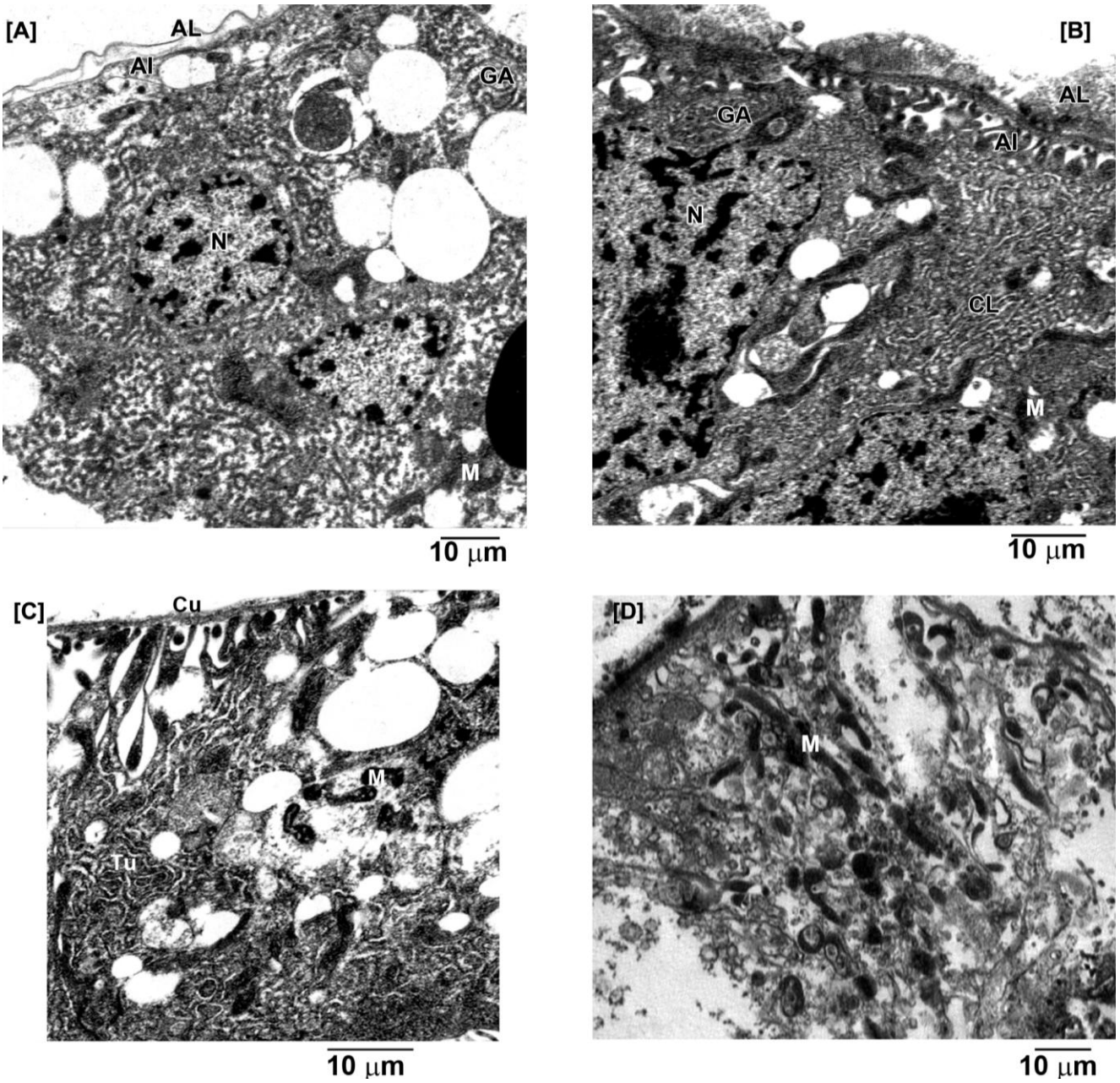

Figure 3. Photomicrograph of TEM of transverse section through the salt gland of nauplii cultured at A, 25 g/L; B, 40 g/L; C, 70 g/L salinity and D, the labryrinth from the previous sector showing a typical mitochondrial pump. AI,Apical infolds; AL, apical layer; CL, cytoplasmic labyrinth; GA, golgi apparatus; M, mitochondria; N, nucleus; R, tubular reticulum.

an abundance of mitochondria with numerous and irregularly arranged cristae. Yolk platelets were completely consumed.

At 180 g/L salinity: The general structure of the salt gland disappeared in *Artemia* cultured at 180 g/L. The cuticle layer became thicker and composed of many layers (Figure 4C). The salt pumps were destroyed and only scattered mitochondria were present and appeared to be separated from each other with less number of cristae (Figure 4D). The apical and central zones showed no amplification of the surface area of the plasma membrane. The labyrinth was absent. Clusters of electron lucent vesicles and membrane bound vesicles of various types were present and occupied the majority of cell. Nuclei were smaller than in other salinities, roughly oval and contain intensely staining nucleoli and chromatin.

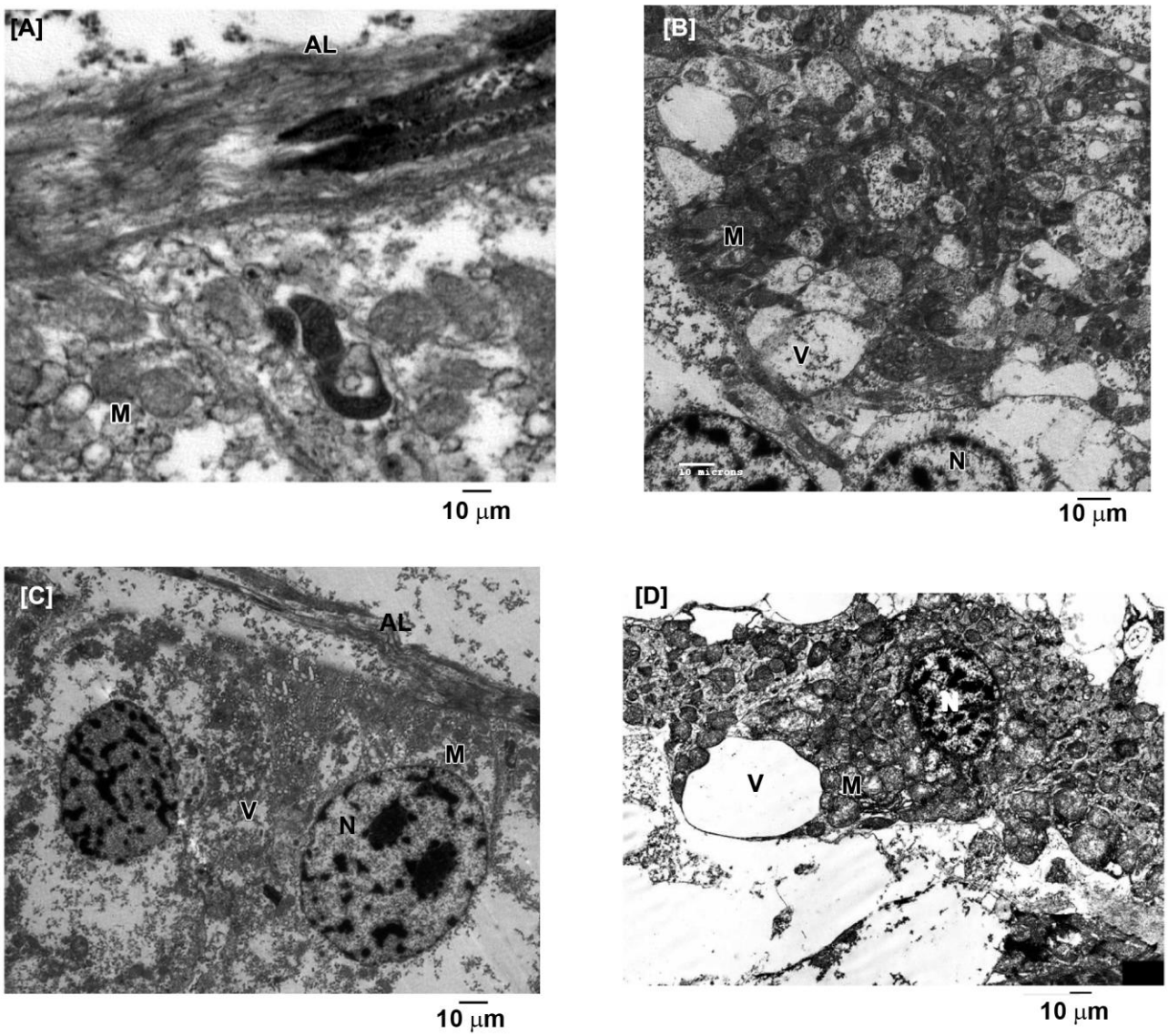

Figure 4. Photomicrograph of TEM of transverse section through the salt glands cultured at A, 140 g/L salinity; B, the basal zone from the previous section showing mitochondria; C, cultured at 180 g/L salinity and D, enlarged portion of the previous section showing the scattered mitochondria. AL, apical layer; M, mitochondria; N, nucleus; V, vacuole.

RT-PCR and analysis of APH-1 gene expression

RT-PCR of mitochondrial 16S rRNA resulted in the amplification of the expected 302 bp fragment in every sample, which indicated the integrity of the total RNA used for RT-PCR as well as the successful first-strand cDNA preparation. Meanwhile, amplification of the APH-1 gave the anticipated 422 bp fragment. In addition, no signal was observed in adult *Artemia* (data not shown) consistent with the lack of APH-1 transcription at this stage.

APH-1 mRNA was expressed in all tested salinities. Low level of expression was noticed in both 25 and 40 g/L salinity concentrations. However, as salinity increased up to 70 g/L the gene was up regulated and higher levels of expression was detected. The APH-1 expression level reached its maximum at 140 g/L salinity. On the other hand, the expression level reduced significantly at salinity 180 g/L (Figures 5 and 6).

DISCUSSION

In the present work, *Artemia* nauplii tolerance to the salinity extremes indicated their proficiency to cope with different NaCl concentrations despite the lack of thoracic appendages and epithelial gut. Under the first four salinities (25, 70, 120 and 140 g/L), *Artemia* was an excellent hypoosmotic regulator; it maintained its low osmotic concentration, not by being very impermeable to water, but by active pumping of NaCl as demonstrated

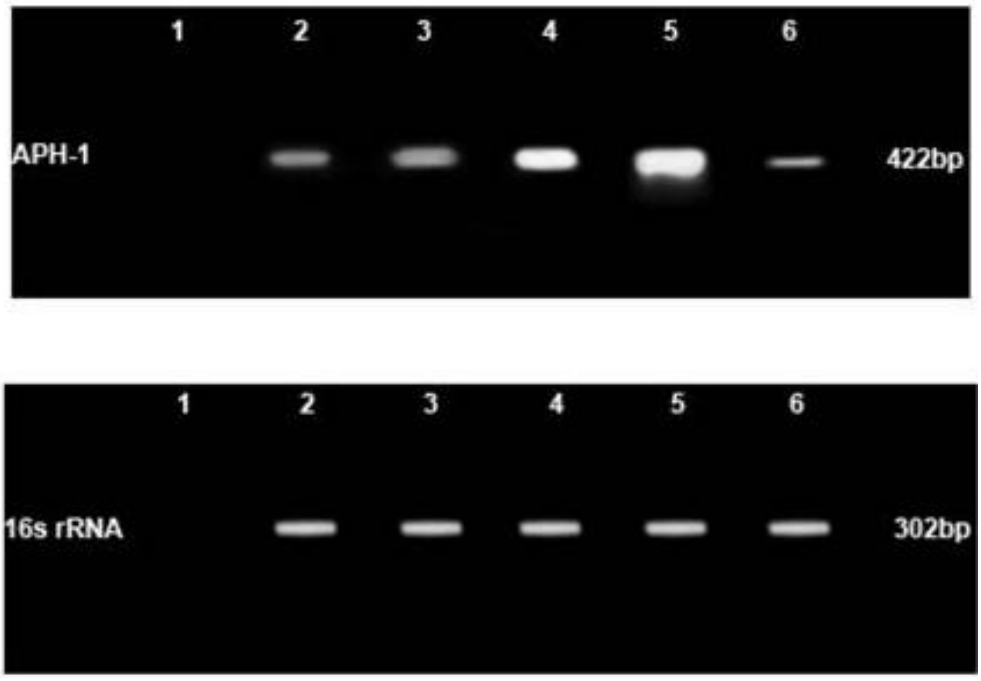

Figure 5. Expression of APH-1 mRNA in *Artemia tunisiana.* Electrophoresis of RT-PCR products of APH-1 (422 bp and 16S rRNA (302 bp) mRNA was performed in ethidium bromide-stained agarose gel (1.5%).Shown are amplicons; lane 1, negative control; lanes 2-6, 25, 40, 70, 140, 180 g/L salinities respectively.

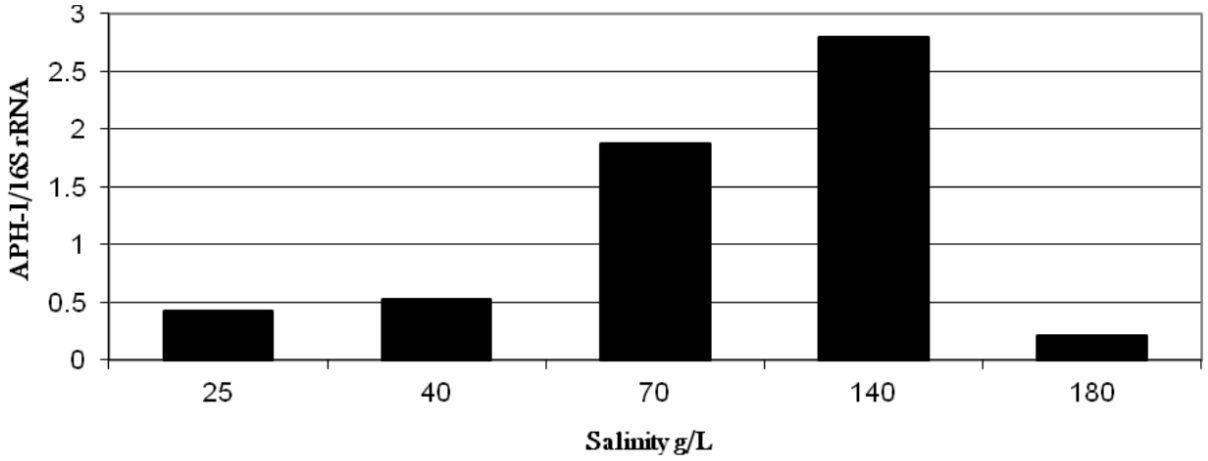

Figure 6. *Artemia tunisiana* APH-1 expression.

from the huge number and distribution of mitochondria and a large amplification of the surface area of the plasma membrane. At 180 g/L salinity *Artemia* survived this treatment but they lost their ability to osmoregulate and became strict osmo conformers.

The present study using scanning electron microscope gave morphological evidence to support the function and adaptation of salt gland due to the different salinities. The shape, size, number of channels and ridges, all of them were influenced by salinity increment. The epithelium with salinity became enlarged may be to engage the new acclimatations as the more amplification of the apical and central zones and the profusion of mitochondria. Also, the hemispherical dome with surface irregularities of epithelium at the high salinities (70, 120, 140 and 180 g/L) incite more surface area for salt excretion. The ultrastructure of the salt gland especially at 40, 70 and 140 g/L was resembled to the branchial gills of the adult.

Hootman and Conte (1975) studied the salt gland ultrastructure and showed its similarity to that of the branchial gills of the adult described by Copeland (1966).

The fine structure of the salt gland in the nauplius confirmed its role in both osmotic and ionic regulation. Ewing et al. (1972) studied the effects of several kinds of inhibitors on survival of nauplii at various salinities and concluded that unusual macromolecular events may be occurring which permit nauplii to live in high concentrations of salt. The modification of the epithelium, the amplification of plasma membrane, and the large populations of mitochondria in the herein species are described in *A. salina* (Hootman and Conte, 1975) and in ion transporting epithelia of other crustaceans as in isopod hindgut (Holdich and Ratcliffe, 1970); the midgut and branchial chamber of the brown shrimp (Talbot et al., 1972); the antennal gland of the fiddler crab (Schmidt-Nielsen et al., 1968); the gills of crabs (Copeland, 1968); and crayfish (Fisher, 1972). The folding of the plasma membrane into an extensive network of tubular reticulum is similar to that observed in the teleost chloride cell (Kessel and Beams, 1962; Karnaky, 1972) and the cells of the avian salt gland (Martin and Philpott, 1973). The amplification of the apical plasmalemma under high salinities (70, 120 and 140 g/L) may serve to increase the surface area available for active solute transport. Also the ramified network of smooth endoplasmic reticulum, which filled the central cytoplasmic zone indicated a salt secretory role of the neck organ under high salinities. Kikuchi (1972) has shown that the extent of smooth tubular network which fills the central cytoplasmic zone (labyrinth) is related to the salinity of the culture medium. The most abundant organelles were mitochondria that also related in their shape, number and size to the degree of salinity. They formed aggregations in intimate contact with the tubular membranes reminiscent of mitochondrial pumps. These mitochondrial pumps were described by Copeland (1967) in the neck organ of *Artemia salina*. Ewing et al. (1972) concluded that the coincident transcription and translation of both nuclear and mitochondrial genes are involved in the development of the naupliar salt gland. *Artemia* at 180 g/L with burnt salt pumps were restricted to narrow range of osmotic regulation. The previous indication is confirmed by the thickness of cuticlular layer in this high salinity concentration in comparison to other tested salinities, which indicated more impermeability to the salt. The survival of these nauplii may be due to the earlier formation of gut (stage 2 instead of 4) than those cultured at lower salinities. The consumption of yolk platelets which contain a unique storage compound in the salt glands of nauplii cultured at 70, 120, 140 and 180 g/L than those cultured at low salinities indicates the high metabolic rate required for nauplii to overcome the high salinities. Also, large quantities of glycogen granules in salt gland at high salinities may provide the cell with metabolic advantages for ATP production.

The most frequent source of evidence for a given protein to be considered relevant in osmoregulation is when its expression or activity is altered after the organism has gone from high to low salt, or vice versa (Saez et al., 2009). Changes in gene expression have been suggested as an important component for adaptation to different environmental conditions and stress management (Schulte 2001; Xu, and Liu, 2011). Several studies examining osmotic pressure stress in animal identify salinity stress through the expression of osmoregulation-related genes (Towle and Weihrauch, 2001; Wu et al., 2011; Barman et al., 2012). Chavez et al. (1999) cloned and sequenced a partial cDNA of *Artemia franciscana* APH-1 (named Af-APH-1). This gene encodes a POU domain family of transcription factors that observed expression in the larvae salt gland but not in the adult *Artemia*. More recently, and by the time of writing up this manuscript, Wang et al. (2012) isolated a full-length cDNAs of *A. sinica* POU-homeoprotein enco-ding gene, designated As-APH-1. The gene encoded a protein of 388 amino acid polypeptide with a calculated molecular mass of 42.85 kDa and an isoelectric point of 6.90 and the protein belongs to the POU III family. The authors determined, by semi-quantitative RT-PCR and whole-mount embryonic immunohistochemistry, an early and persistent expression of As-APH-1 in the naupliar stages, which suggests that As-APH-1 functions very early in the salt gland and may be required continuously in this organ, while later in development, the expression of the gene begins to dramatically decrease and disappear in salt gland and appears in the thoracic epipods in sub-adult. In addition, they tested the expression under different salinities (50, 75, 100, 125 and 150 g/L) and realized that As-APH-1 increased obviously as the salinity increased, with almost no expression in 50 g/L, initial increase in expression in 75 g/L, constantly increase in 100 g/L and a highest expression level was reached in 150 g/L salinity. In the present study, APH-1 mRNA was expressed in all tested salinities. Contrary to Wang et al. (2012), detectable level of expression was noticed in both 25 and 40 g/L salinity. As salinity increased up to 70 g/L the gene was up regulated and higher level of expression was detected. The APH-1 expression level reached its maximum at 140 g/L salinity. On the other hand, the expression was reduced significantly at salinity 180 g/L, which demonstrates that the nauplii became less capable of coping with greatly increased salt load. This reduction in gene expression also concurs with the recorded structure diminishing of the salt gland in this salinity concentration.

In conclusion, *Artemia* represents a valuable model for a salinity tolerated organism. Our results demonstrate differences in the morphology and structure of *A. tunisiana* salt gland as well as in the expression of APH-1 reflecting salinity changes. Although it can be used as a good indicator of salinity stress, the observation that this expression is lowered in the highest tested salinity, with *Artemia* ability to withstand very high salinity concentra-

tions, highlights the possible contribution of other gene(s) to compensate this salinity augment. As the mechanism of adaptability to hypersaline water is expected to be a complex physiological and molecular process, further investigation of this issue is auspicious.

REFERENCES

Abel JH, Ellis RA (1966). Histochemical and electron microscopic observations on the salt secreting lachrymal glands of marine turtles. Amer. J. Anat.118:337-358.

Anderson MG, Certel SJ, Certel K, Lee T, Montell DJ, Johnson WA (1996). Function of the Drosophila POU domain transcription factor drifter as an upstream regulator of breathless receptor tyrosine kinase expression in developing trachea. Development 122:4169-4178.

Barman HK, Patra SK, Das V, Mohapatra SD, Jayasankar P, Mohapatra C, Mohanta R, Panda RP, Rath SN (2012). Identification and characterization of differentially expressed transcripts in the gills of freshwater prawn (*Macrobrachium rosenbergii)* under salt stress. The Sci. W. J.

Bell AL, Barnes SN, Andrson KL (1969). A fixation technique for electron microscopy which provides uniformly good preservation of the tissues of a variety of marine invertebrates. Biol. Bull. 137:393.

Chavez M, Landry C, Loret S, Muller M, Figueroa J, Peers B, Rentier-Delrue F, Rousseau GG, Krauskopf M, Martial JA (1999). APH-1, a POU homeobox gene expressed in the salt gland of the crustacean *Artemia franciscana*. Mech. Dev. 87:207-212.

Conte FP, Droukas PC, Ewinf RD (1977). Development of sodium regulation and *de novo* synthesis of Na+K-activated ATPase in the larval brine shrimp *Artemia salina*. J. Exp. Zool. 202:339-361.

Conte FP, Hootman SR, Harris PJ (1972). Neck organ of *Artemia salina* nauplii: a larval salt gland. J. Comp. physiol. 80:239-246.

Copeland DE (1966). Salt transport organelle in *Artemia salenis* (brine shrimp). Science. 151:470-471.

Copeland DE (1967). A study of salt-secreting cells in the brine shrimp (*Artemia salina*). Protoplasma, 63:363-384.

Copeland DE (1968). Fine structure of salt and water uptake in the land crab, *Gecarcinus lateralise*. Amer. Zool. 8:417-432.

Criel RJ (1991). Morphology of *Artemia*. In, *Artemia* biology. (Brown RA, Sorgeloos, P , CNA Trotman, eds) CRC Press, Boca Raton, FL, Pages 155-185.

Croghan PC (1958). The mechanism of osmotic regulation in *Artemia salina* (L.): the physiology of the gut. J. Exp. Biol. 35:243-249

Dejdar E (1930). Die Korrelationen zwischen Kiiemensackchen und Nackenschild bei phyllopoden. (Versuch einer Analyse mit Hilfe elective vitalfarbung.) Z. wiss. Zool. 136:422-452.

Ewing RD, Peterson GL, Conte FP (1972). Larval salt gland of *Artemia salina* nauplii. Effects of inhibitors on survival at various salinities. J. Comp. Physiol. 80:247-254.

Ewing RD, Peterson GL, Conte FP (1974). Larval salt gland of *Artemia salina* nauplii: localization and characterization of sodium and potassium-activated adenosine triphosphatase. J. Comp. Physiol. 88:217-234.

Fisher JM (1972). Fine-structural observations on the gill filaments of the freshwater cryfish *Astacus pallipes* Lereboullet. Tissue and cell, 4:287-299.

Fryer G (1987). A new classification of the branchiopod Crustacea. Zool. J. Linn. Soc. 91:357-383.

Holdich DM, Ratcliffe NA (1970). A light and electron microscopic study of the hindgut of the herbivorous isopod, *Dynamene bidentata* (crustacean: pericarida). Z. Zellforsch., 111:209-227.

Hootman SR, Conte FP (1975). Functional morphology of the neck organ in *Artemia salina* nauplii. J. Morph. 145(3):371-386.

Hootman SR, Harris PJ, Conte FP (1972). Surface specialization in the larval salt gland in *Artemia salina* nauplii. J. Comp. Physiol.79:97-104.

Karnaky KJ (1972). Osmoregulation in euryhaline teleosts: cytological and biochemical studies on the branchial epithelium of *Cyprinodon variegateus*. PhD Thesis. Rice University. Houston, Texas.

Kessel RG, Beams HW (1962). Electron microscopic studies on the gill filaments of *fundulus heteroclitus* from sea water and fresh water with special reference to the ultrastructural organization of the “chloride cell”. J. Ultr. Res. 6:77-87.

Kikuchi S (1972). Three-dimensional network of a tubular system in the salt-transporting cells of the gill and the neck organ of *Artemia salina* (brine shrimp). Annual Report of the Iwate Medical University school of Liberal Arts and Science 7:15-22.

Martin BJ, Philpott CW (1973). The adaptive response of the salt glands of adult mallard ducks to a salt water regime: an ultrastructural and tracer study. J. Exp. Zool. 186:111-122.

Martin JW, Laverack MS (1992). On the distribution of the crustacean dorsal organ. Acta Zoologica 73:357-368.

Palmero I, Renart J, Sastre L (1988). Isolation of cDNA clones for mitochondrial 16S ribosomal RNA from the crustacean *Artemia*. Gene 68:239-248.

Russler D, Mangos J (1978). Micropuncture studies on the osmo-regulation in the nauplius of Artemia salina. American J. Physiol. 234:R216-R222.

Sáez AG, Lozano E, Zaldívar-Riverón A (2009). Evolutionary history of Na, K-ATPases and their osmoregulatory role. Genetica. 136 (3):479-490.

Sars GO (1896). Fauna Norvegiae, Vol. I. Descriptions of the Norwegian species at present known belonging to the suborders Phyllocarida and Phyllopoda. Joint-stock, Christiania.

Schmidt-Nielsen B, Gertz HK, Davis LE (1968). Excretion and ultrastructure of the antennal gland of the fiddler crab, Uca modax. J. Morph. 125:473-496.

Schrehardt A (1986). Der Salinenkrebs Anemia 2. Die postembryonale Entwicklung- Mikrokomos 75:334-340.

Schrehardt A (1987). A scanning electron-microscopic study of the post-embryonic development of *Artemia*. In *Artemia*: Research and Applications, Volume 1, (P. Sorgeloos et al., eds), Universa Press, Wetteren, Belgium, pp.5-32.

Schulte PM (2001). Environmental adaptations as windows on molecular evolution. Comp. Biochem. Physiol. B. Biochem. Mol. Biol. 128:597-611.

Sorgeloos P (1978). The culture and use of brine shrimp *Artemia salina* as food for hatchery raised larval prawns, shrimp and fish in South East Asia. FAO Report THA/75/008/78/WP3, 50pp.

Talbot PW, Clark HJ, Lawrence AL (1972). Fine structure of the midgut epithelium in the developing brown shrimp, *Penaeus aztecus*. J. Morph. 138:467-486.

Towle DW, Weihrauch D (2001). Osmoregulation by gills of euryhaline crabs: molecular analysis of transporters. Amer. Zool. 41:770-780.

Varo I, Navarro JC, Amat F, Guilhermino L (2002). Characterization of cholinesterases and evaluation of the inhibitory potential of chlorpyrifos and dichlorvos to *Artemia salina* and *Artemia parthenogenetica*. Chemosphere 48:563-569

Wang JQ, Hou L, Yi N, Zhang RF, Zou XY (2012). Molecular analysis and its expression of a pou homeobox protein gene during development and in response to salinity stress from brine shrimp, *Artemia sinica*. Comp. Biochem. Physiol. 161(A):36-43.

Weisz PB (1947). The histological pattern of metameric development in *Artemia salina*. J. Morph. 81:45-95.

Wu G, Zhang H, Sun J, Liu F, Ge X, Chen WH, Yu, J, Wang W (2011). Diverse LEA (late embryogenesis abundant) and LEA-like genes and their responses to hypersaline stress in post-diapause embryonic development of *Artemia franciscana*. Comp. Biochem. Physiol. 160(B):32-39.

Xu Q, Liu Y (2011). Gene expression profiles of the swimming crab *Portunus trituberculatus* exposed to salinity stress. Mar. Biol. DOI 10.1007/s00227-011-1721-8.

Zelzer E, Shilo BZ (2000). Interaction between the bHLH-PAS protein Trachealess and the POU-domain protein drifter specifies tracheal cell fates. Mech. Dev. 91:163-173.

Zenker W (1851). Physiologische bemerkungen uber die Daphnoiden. Arch. Anat. Physiol. Med. 1851:112-121.